ORIGINAL PAPER

Effect of weakening of sliding zone soils in hydro-fluctuation belt on long-term reliability of reservoir landslides

Kang Liao[1] · Yiping Wu[1] · Fasheng Miao[1] · Linwei Li[1] · Yang Xue[1]

Abstract

The impoundment of the Three Gorges Reservoir in China inevitably caused the reservoir landslides to develop toward instability, which has attracted widespread attention. Taking the Huangtupo Riverside Slump 1# with the structural characteristics of double sliding zones as a case, this study focuses on the sliding zone soils in the hydro-fluctuation belt affected by the periodic fluctuations of reservoir water level. The wetting-drying cycles test is carried out to simulate the cyclic impact of the fluctuations on the sliding zone soils. Hence the weakening law of the strength parameters is illustrated and well characterized by an exponential function model. Considering the different number of wetting-drying cycles, the long-term reliability of the shallow and deep sliding surfaces is quantified via the imbalance thrust force method and reliability theory. The results indicate that the local failure probability of both sliding surfaces gradually rises as the number of wetting-drying cycles increases. In particular, the shallow sliding surface presents a greater local failure probability than that of the deep one since more slices are in the hydro-fluctuation belt. Besides, the sensitivity of the landslide response to the strength parameters is different, and the internal friction angle is much greater than the cohesion. The area of the hydro-fluctuation belt plays a significant role on the long-term reliability of the landslide, which should be closely monitored to guide the reservoir operation.

Keywords Reservoir landslides · Hydro-fluctuation belt · Wetting-drying cycles · Long-term reliability · Imbalance thrust force method · Reliability theory

Introduction

The occurrence of catastrophic landslides has the potential not only to cause heavy casualties and property losses but also to bring irreparable damage to resources, environment, and ecology (Huang 2009; Kirschbaum et al. 2015; Yin et al. 2016). In recent

✉ Yiping Wu
   ypwu@cug.edu.cn

   Kang Liao
   Kangliao@cug.edu.cn

   Fasheng Miao
   fsmiao@cug.edu.cn

   Linwei Li
   linweili93@126.com

   Yang Xue
   egxyang@163.com

[1] Faculty of Engineering, China University of Geosciences, Wuhan 430074, China

decades, with the rapid increase of clean energy demand and the substantial enhancement of natural transformation ability, a growing number of infrastructure projects, including large hydropower stations, have been built in mountainous areas (Duman 2009; Huang 2012). As a result, many landslides located in the reservoir area occur as the reservoir-induced landslides (Paronuzzi et al. 2013; Yin et al. 2016; Tang et al. 2019). Since the Vajont landslide disaster in 1963, reservoir landslides have attracted close attention due to its characteristics of wide distribution, strong suddenness, high frequency, and great harm (Barla and Paronuzzi 2013). Therefore, research on reservoir landslides, with a focus on analyzing the influence of periodic reservoir operations and evaluating the long-term stability, is an imperative issue worldwide.

The Three Gorges Hydropower Station on the Yangtze River in China has the largest installed hydropower capacity in the world. The periodic operations of reservoir water level have evidently increased the frequency of geological disasters, especially landslides (Tang et al. 2019). According to statistics, there are more than 5300 landslides along the reservoir bank of about 2000 km in the Three Gorges Reservoir Area

(TGRA), and more than 60 landslides have been triggered by the reservoir operations (Du et al. 2013; Yao et al. 2020). Furthermore, the periodic fluctuations of reservoir water level have awakened some large-scale ancient landslides with multiple sliding zones to be reactivated and even destroyed (Gutiérrez et al. 2010; Micu and Bălteanu 2013; Wang et al. 2018a). An extreme case is the destructive Qianjiangping landslide, which occurred 14 days after the reservoir impounded from 95 to 135 m in 2003, killing 24 people and destroying 346 houses (Yin et al. 2016; Tang et al. 2019).

The filling of the TGRA has a cyclical fluctuation of 30 m (145–175 m) to meet the demands of flood control and power generation, which results in an observable hydro-fluctuation belt (Deng et al. 2016; Liao et al. 2020a). When the reservoir water level rises, the soils in this belt are in a saturated state by the water supply; on the other hand, when the level of the reservoir drops, the piezometric level (or groundwater level) also drops thanks to the drainage devices on the landslide. The water content can vary above this piezometric surface. However, it varies very little in soils with a clay component. In fact, a capillary fringe is established above the piezometric surface at which the soils remain saturated. This capillary fringe can develop over great heights. Consequently, the study carried out in this article is partly theoretical because it makes the assumption of a variation of water contents at the level of the surfaces of failure. Only samples at the level of these failure surfaces, for the different piezometric levels, could clarify this subject. In this case, the earth mass in this belt experiences repeated wetting-drying cycles due to the periodic reservoir operations, leading to changes in its composition, structure, and properties (Gullà et al. 2006; Ng et al. 2009; Tang et al. 2016; Pasculli et al. 2017). As a result, the alternating wetting-drying processes are likely to cause the deterioration of the soil strength and urge the disintegration of the soil structure.

It is widely recognized that the sliding zone plays a key role in controlling the landslide deformation (Wen et al. 2007; Tang et al. 2015a). Hence the weakening way of the sliding zone soils and the effect of this weakening on the stability of the landslide have been closely concerned (Penna et al. 2013; Deng et al. 2017; Jiang et al. 2019; Miao et al. 2020). Currently, most of the studies contain only a single sliding zone, and little attention is paid to multiple sliding zones while considering the influence of the hydro-fluctuation belt simultaneously. Therefore, it is necessary to analyze the complex landslide with multiple sliding zones and quantify the weakening of sliding zone soils in the hydro-fluctuation belt under long-term reservoir operations, so that the comprehensive performance of the landslide can be understood.

There is an ever-increasing interest in analyzing the structural stability from a probabilistic point of view (Chen et al. 2019). Reliability theory is a probability calculation method developed in recent decades, which has been widely used in structural engineering, and landslides are no exception (Phoon et al. 2013; Li et al. 2015; Fenton et al. 2016; Juang et al. 2018). In conventional stability analysis, the factor of safety is an index to evaluate the landslide state assuming that the geotechnical properties are invariable. In fact, uncertainties are an inherent property of geotechnical properties (gravity, cohesion, internal friction angle, permeability coefficient, etc.), which vary within a given range of variation (Peng et al. 2017). Therefore, considering the variability of geotechnical properties is of great significance for landslide stability analysis.

This study aims to evaluate the long-term reliability of the reservoir landslides by considering the weakening of the sliding zone soils in the hydro-fluctuation belt. The Huangtupo Riverside Slump 1# which has the structural characteristics of double sliding zones in the TGRA is selected as the case study. The wetting-drying cycles test is conducted to simulate the weakening of sliding zone soils in the hydro-fluctuation belt under the repeated reservoir operations, and an exponential model is proposed to outline the degradation. In addition, the imbalance thrust force method and reliability theory are introduced to analyze the stability and local failure probability of the landslide. Then, the long-term reliability of the Riverside Slump 1# is quantified and discussed based on weakening of sliding zone soils in hydro-fluctuation belt under wetting-drying cycles.

Materials

Geological setting

The Huangtupo landslide in the TGRA is located on the south bank of the Yangtze River in Badong County, Hubei Province, about 2 km from the Badong Bridge (Fig. 1a). The Huangtupo landslide is developed in the limestone and argillaceous limestone with weak interlayers of the Middle Triassic Badong Formation (T$_2$b). The materials of the sliding mass are primarily rock and soil debris, which are originating from the weathering of the bedrock, water-rock interaction, and down slope transportation. Four subordinate landslides make up this massive landslide, which are called Riverside Slump 1#, Riverside Slump 2#, Substation Landslide, and Garden Spot Landslide (Fig. 1b). The composite landslide is famous for its huge scale, complex structure, diverse causes, serious hazards, and difficult governance, so it has become the most noticeable reservoir landslide in the TGRA (Tang et al. 2015b). Geometrically, this mass covers an area of 1.35 km^2, with a volume of nearly 70 million m^3, forming the largest reservoir landslide in China.

Previous studies combined with field investigation and monitoring data have demonstrated that the Riverside Slump 1# has the highest risk of instability among the four
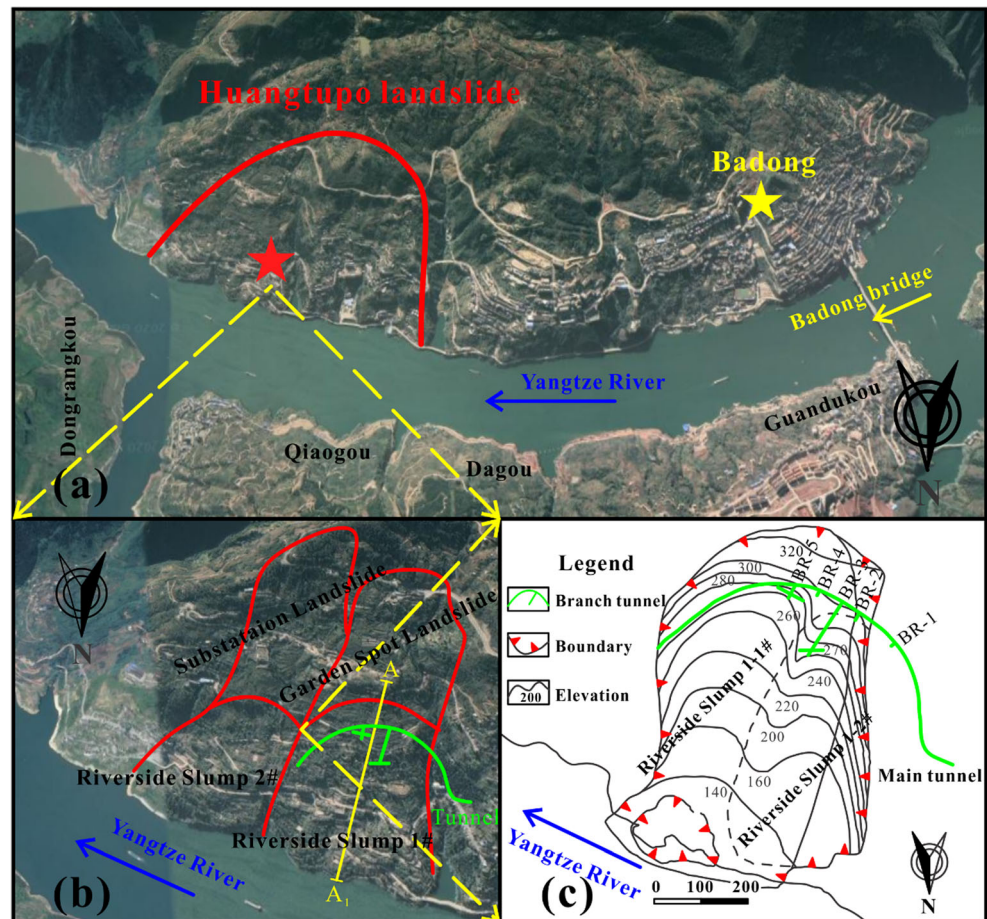
subordinate landslides in the Huangtupo landslide (Wang et al. 2018a; Li et al. 2019). Therefore, in order to comprehensively expose the structure characteristics and evolution mechanism of the Riverside Slump 1#, a large-scale tunnel group that consists of a main tunnel and five branch tunnels with a series of in situ monitoring systems was constructed for further analysis (Tang et al. 2015a).

The borehole coring and inclinometer monitoring data suggest that the Riverside Slump 1# has the structural characteristics of double sliding zones (Wang et al. 2018b). The deep sliding zone exposed by the main tunnel and BR-5 is located at the contact surface between the bedrock and the sliding mass, and the elevation of the shear outlet is about 60 m. The thickness of the sliding zone between the bedrock and the sliding mass is 0.1 to 0.3 m, which is composed of grayish-green silty clay and gravels. Another shallow sliding zone developed on the western boundary of the Riverside Slump 1# is revealed by the BR-3, and the elevation of the shear outlet is about 90 m. Different from the materials of the sliding zone in the main tunnel and BR-5, the color of the soils here is brownish yellow instead of grayish-green, and a finer particle size with less gravels is observed. Furthermore, the U-Th dating method was conducted to test the calcite samples of the sliding zones collected from BR-3 and BR-5, and the

indicated age results were 40 and 100 ka, respectively (Wang et al. 2018b). These clues confirm that the sliding zones in BR-3 and BR-5 are in different sliding surfaces (Tang et al. 2015a; Wang et al. 2018b). Therefore, two sliding surfaces exist in the east and west of the Riverside Slump 1#, respectively, which divide the Riverside Slump 1# into two secondary landslides, named the Riverside Slump 1-1# and Riverside Slump 1-2# (Fig. 1c). Taking A-A' (Fig. 1b) as the baseline, the cross section is shown in Fig. 2, in which the deep sliding surface is marked in red and the shallow sliding surface is marked in green.

Hydrogeological setting

Badong County, where the Huangtupo landslide is located, belongs to the subtropical monsoon region, with four distinct seasons and abundant rainfall. According to statistics, the annual average temperature in the landslide area is 17.5 °C, of which July and August are high-temperature periods each year with an average daily temperature of 35.3 °C and January and February are low-temperature periods with an average daily temperature of 3.8 °C. The average rainfall in the landslide area is 1100.7 mm, and the period of concentrated rainfall is
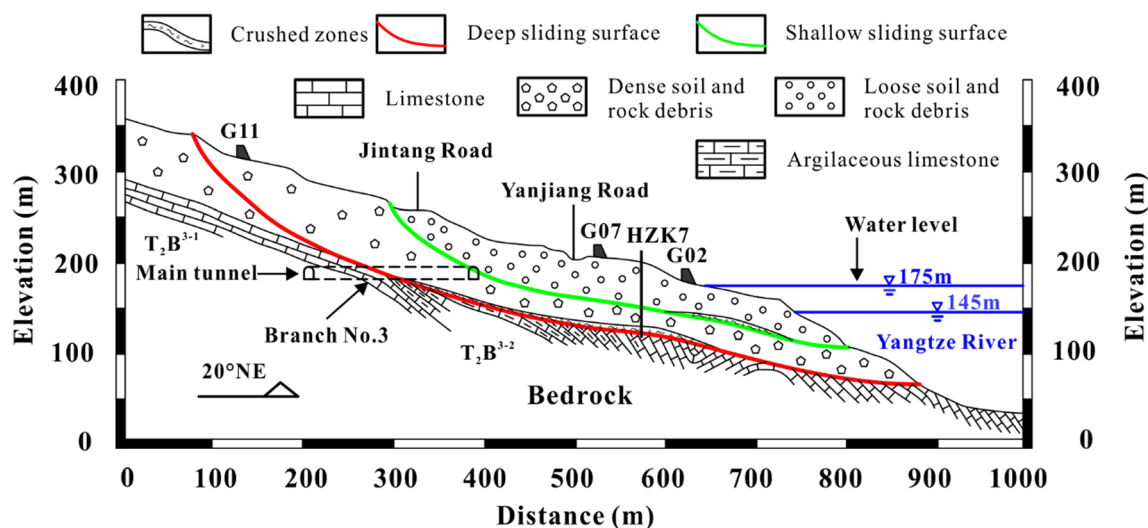
Fig. 2 Schematic geologic cross section of the Riverside Slump 1# (revised from Ni et al. 2013)

from April to September, which can reach 71.8% of the annual rainfall.

As illustrated in the geologic cross section (Fig. 2), the shallow sliding mass of the Huangtupo Riverside Slump 1# is composed of loose soil and rock debris, which has been tested to have good permeability (Wang et al. 2014). According to the demands of reservoir scheduling, the water level of the TGRA cyclically rises and falls between 175 and 145 m annually, resulting in a typical hydro-fluctuation belt with a height difference of 30 m. The fluctuation of reservoir water level inevitably causes the change of the groundwater level, which has a significant influence on the deformation of the landslide. In order to interpret the relationship between the reservoir water level and the groundwater level, borehole HZK7 was installed, and the recorded results were shown in Fig. 3.

It can be seen from Fig. 3 that the groundwater level fluctuates with the scheduling of the reservoir water level. When the reservoir water level rises, the reservoir water supplements the groundwater, causing the groundwater level to rise
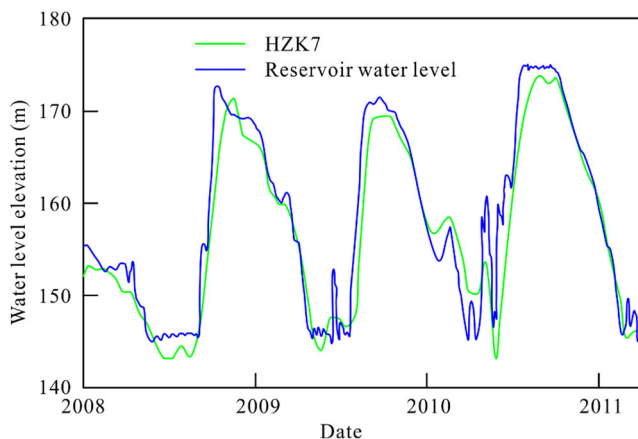
accordingly; when the reservoir water level falls, on the other hand, the groundwater in turn supplements the reservoir water, causing the groundwater level to drop.

As a result, the soils located in the hydro-fluctuation belt register variations in pore water pressure, and we postulate that this follows variations in water content (from a saturated state to an unsaturated state) with, consequently, variations in mechanical parameters, which are the main contribution of this article. Although the weakening is usually a gradual process and the effect of each cycle may not be obvious, the results will be amplified after repeated interactions, conclusively causing the failure.

Wetting-drying cycles test

In order to investigate the weakening law of the sliding zone soils, the wetting-drying cycles test is performed, which artificially generates the alternating process, reducing the time needed naturally, through more intense cycles of weakening.

The materials used in this test program are sampled from the BR-3 of the Riverside Slump 1#, which are mainly composed of silty clay with gravel and debris in a reservoir environment (Fig. 4). Four samples are tested, and the average physical parameters are measured as shown in Table 1.

The samples are divided into five groups, six for each group, corresponding to the number of wetting-drying cycles. In this test, a complete wetting-drying cycle includes two processes, air-drying and saturation, of which the air-drying process is reached by evaporating the samples in natural conditions and the saturation process is completed by soaking in an aspirator. Throughout the article, for simplicity, the term "wetting-drying cycles" is employed. In reality it should be understood that the change of the mechanical characteristics of sliding zone soils with water content is the essence of this study. The change range of the moisture content herein is set

Fig. 3 Fluctuation of the water level in the Three Gorges Reservoir and groundwater level in the borehole HZK7 (revised from Tang et al. 2015b)

Table 1 Average physical parameters of the sliding zone soil

Natural weight γ_n (kN/m^3)	Dry weight γ_d (kN/m^3)	Natural moisture content W (%)	Saturation S_r (%)	Liquid limit W_L (%)	Plastic limit W_P (%)	Plastic index I_P
20.30	17.90	15.97	75.5	25.95	13.86	12.09

between 10 and 21% based on the physical properties of the samples and its storage environment. The maximum 21% is the saturated moisture content, while the minimum 10% is determined on the basis of the annual variation of water content in the sliding zone soils (Lu et al. 2018; Miao et al. 2020). The realization of the whole cycle process is completed by weighing at 60-min intervals.

Furthermore, the TYS-500 triaxial shear test apparatus is employed to conduct the consolidated undrained test (CU). The prepared samples are tested under the confining pressures of 100, 200, 300, and 400 kPa, respectively, and the shear rate is controlled at 0.8 mm/min during the shearing process. The test can be terminated until the load reaches the peak strength of the samples. Alternatively, the strain of 15% can be considered as the damage point if the peak shear strength is not observed. In this way, the normal stress (σ) and the shear strength (τ) of the samples can be acquired by Eq. (1).

$$\begin{cases} \sigma = \dfrac{1}{2}(\sigma_1 + \sigma_3) + \dfrac{1}{2}(\sigma_1 - \sigma_3)\cos 2\alpha \\ \tau = \dfrac{1}{2}(\sigma_1 - \sigma_3)\sin 2\alpha \\ \alpha = 45° + \dfrac{1}{2}\varphi \end{cases} \quad (1)$$

Taking the initial state of samples as an example (0 wetting-drying cycle), the strain-stress curves under different confining pressures and the corresponding strength envelope diagrams are shown in Fig. 5.

Subsequently, the cohesion (c) and internal friction angle (φ) are obtained based on the relationship between σ and τ (Fig. 5b). As shown in Table 2, the peak strength increases with the increase of confining pressure, which is opposite to the number of wetting-drying cycles. Similarly, the strength parameters show a decreasing tendency with increasing wetting-drying cycles, especially φ. But c appears a certain increase at the beginning of the test. A reasonable interpretation for this phenomenon is that the hydrophilic materials are included in the sliding zone soils, such as montmorillonite and illite (Jiao et al. 2014). When the sample is saturated, these materials swell with water to fill the gaps and cement the debris, so an increase in c is observed. After several cycles, the reinforcing effect is reduced, and the mechanical weakening gradually appears. As a result, the observed increase is time-sensitive.

100, 200, 300, and 400 kPa are the confining pressure

Methods

Failure mechanism model

Limit equilibrium methods for assessing the stability of landslides are commonly used in engineering practice due to its simple principles and effective outcomes. To date, many researchers have established different equilibrium equations and

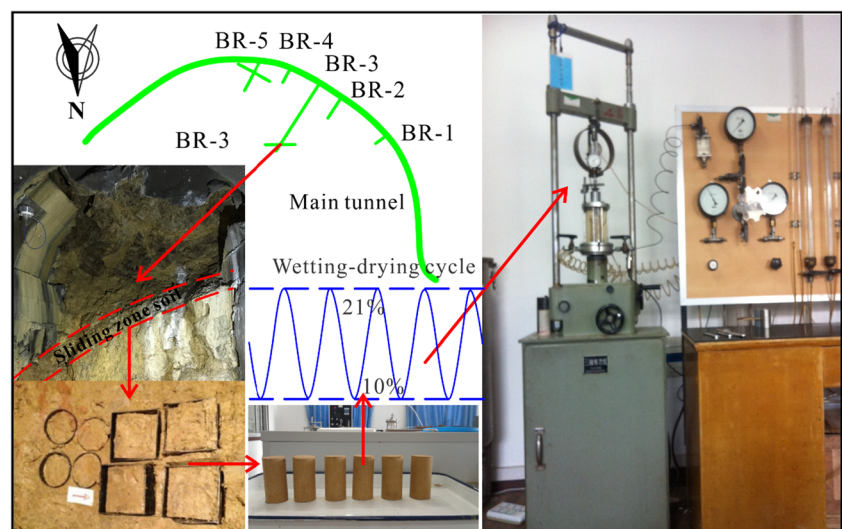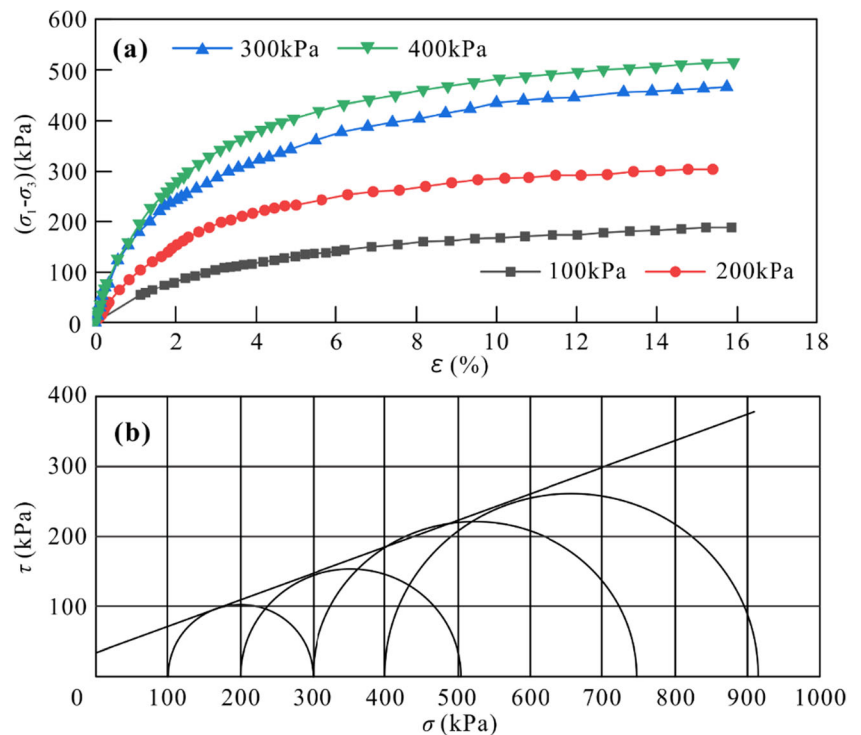**Fig. 4** Sampling position and experimental instrument of the sliding zone soils

Fig. 5 a The strain-stress curves from the triaxial test, **b** the strength envelope diagram from the triaxial test

relationship assumptions between the interslice shear and normal forces to enrich the limit equilibrium fundamentals (Bishop 1955; Janbu 1957; Morgenstern and Price 1965; Spencer 1968; Sarma 1979; Zhu et al. 1999). Among these techniques, the imbalance thrust force method proposed by Zhu et al. (1999) has been recognized as one of the most popular ways, especially in China. It is an improved Janbu method assuming that the direction of the force between the slices is consistent with the inclination of the slices, while the direction in Janbu method is taken to be horizontal.

As shown in Fig. 6a, a typical reservoir landslide with double sliding surfaces is illustrated. When analyzing the shallow sliding surface, the sliding mass is divided into n slices, of which the sliding force is T_i and the anti-sliding force is R_i. The free body diagram gives an indication as to where the forces act on the ith slice (Fig. 6b). According to the force equilibrium, T_i and R_i can be expressed as follows:

$$T_i = (W_{i1} + W_{i2})\sin\alpha_i + F_{i-1}\cos(\alpha_{i-1}-\alpha_i)_i - F_i + D_i\cos(\beta_i-\alpha_i) \tag{2}$$

$$R_i = [(W_{i1} + W_{i2})\cos\alpha_i + F_{i-1}\sin(\alpha_{i-1}-\alpha_i) + D_i\sin(\beta_i-\alpha_i)]\tan\varphi_i + c_i l_i \tag{3}$$

where W_{i1} and W_{i2} denote the natural gravity and effective gravity of the ith slice, respectively; α_i denotes the ground inclination of the ith slice; F_{i-1} denotes the residual thrust from the first to i-1th slice acting on the ith; F_i denotes the capacity of maximum support force that can be provided by the slices from i+1th to nth; D_i denotes the osmotic pressure of the ith slice and can be quantified by $W_{wi}\sin\beta_i$, in which W_{wi} denotes the water gravity of the ith slice and β_i denotes the angle between the phreatic line of the ith slice and the horizontal plane; c_i and φ_i denote the cohesion and internal friction angle of the ith slice, respectively; and l_i denotes the length of the ith slice on sliding surface.

Table 2 Peak strength and average strength parameters under wetting-drying cycles

Number of cycles	Peak strength(kPa)				Strength parameters	
	100 kPa	200 kPa	300 kPa	400 kPa	c (kPa)	φ (°)
0	190.41	304.29	467.08	515.8	31.81	21.46
1	182.15	292.60	392.08	452.88	36.42	18.31
2	169.82	277.21	326.78	410.29	38.41	16.22
3	145.10	248.22	301.79	385.81	28.32	16.27
4	137.85	229.91	275.66	354.24	28.81	14.99

Fig. 6 **a** Diagram showing slices of a reservoir landslide with double sliding surfaces, **b** forces acting on the shallow slices, **c** forces acting on the deep slices
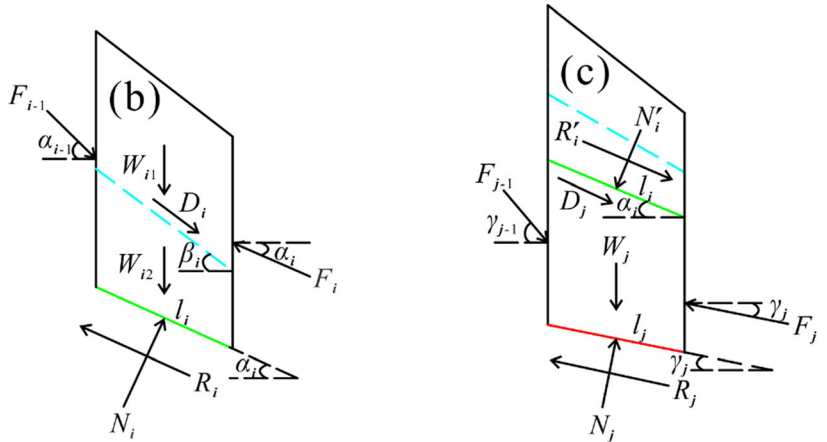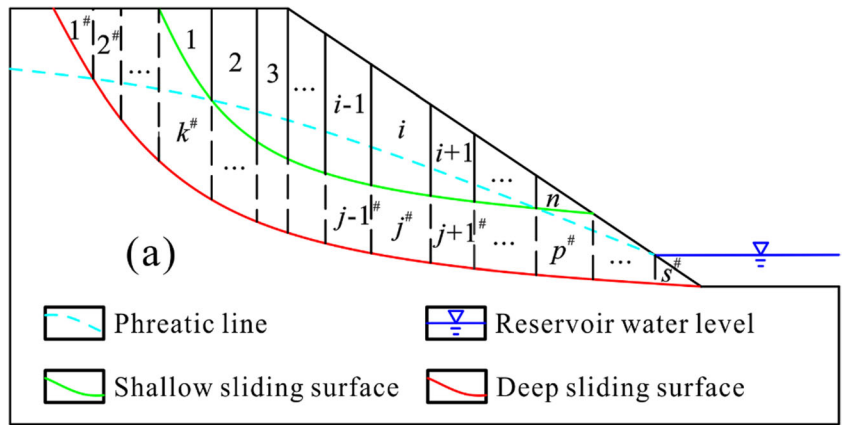
Let F_s denote the factor of safety, which can be answered by the iteration method (Yao et al. 2020). Then, F_i can be expressed as:

$$\begin{cases} F_1 = F_{i-1}\psi_i + (W_{i1} + W_{i2})\sin\alpha_1 + D_1\cos(\beta_1-\alpha_1)-(c_il_i + M_i\tan\varphi_i)/F_s \\ \psi_i = \cos(\alpha_{i-1}-\alpha_i)-\sin(\alpha_{i-1}-\alpha_i)\tan\varphi_i/F_s \\ M_i = (W_{i1} + W_{i2})\cos\alpha_i + D_1\sin(\beta_1-\alpha_1) \end{cases}$$

$$(4)$$

where ψ_i denotes the transfer coefficient of imbalance thrust from the i-1th slice to the ith slice.

On the other hand, the deep sliding mass is divided into s slices, of which the kth and pth slices are connected with the first and nth slices of the shallow sliding mass. The impacts of upper sliding mass can therefore be considered to the equivalent forces exerting on the shallow sliding surface (Fig. 6c). Further, the equivalent forces can be decomposed according to the direction of the deep sliding surface as:

$$U_j = R_i'\cos\left(\alpha_i-\gamma_j\right)-N_i'\sin\left(\alpha_i-\gamma_j\right) \quad (5)$$

$$V_j = R_i'\sin\left(\alpha_i-\gamma_j\right) + N_i'\cos\left(\alpha_i-\gamma_j\right) \quad (6)$$

$$R_i' = -\{[(W_{i1} + W_{i2})\cos\alpha_i+F_{i-1}\sin(\alpha_{i-1}-\alpha_i)+D_i\sin(\beta_i-\alpha_i)]\tan\varphi_i+c_il_i\}$$

$$(7)$$

$$N_i' = -[(W_{i1} + W_{i2})\cos\alpha_i+F_{i-1}\sin(\alpha_{i-1}-\alpha_i)+D_i\sin(\beta_i-\alpha_i)] \quad (8)$$

where R_i' and N_i' correspond to R_i and N_i, respectively, with the same values but opposite directions, and N_i denotes the base normal force of the ith slice.

Analogously, F_j can be calculated as:

$$F_j = F_{j-1}\psi_j + \left(W_{j1} + W_{j2}\right)\sin\alpha_j + D_j\cos\left(\beta_j-\alpha_j\right)$$
$$+ U_j-\left[c_jl_j + \left(M_j + V_j\right)\tan\varphi_j\right]/F_s' \quad (9)$$

Reliability theory

In general, the factors that affect the structural function can be summarized as load (T) and resistance (R). In this way, the function that characterizes the structural performance can be expressed as:

$$Z = R-T \quad (10)$$

This expression is also applicable to the landslide, which can be described as the relationship between the sliding force and anti-sliding force. As a result, three equations may result:

$$\begin{cases} Z = R-T > 0, \text{ Stable} \\ Z = R-T = 0, \text{Limit equilibrium} \\ Z = R-T < 0, \text{Failure} \end{cases} \quad (11)$$

Table 3 Statistical data of strength parameters under wetting-drying cycles

Sources	Parameters	Number of wetting-drying cycles						
		0	1	2	3	4	5	6
Jiang et al. (2019)	c	31.42	20.95	15.47	10.21	5.84	4.37	4.46
	φ	26.97	26.39	26.44	25.95	25.24	25.04	24.61
Deng et al. (2017)	c	18.32	15.58	13.21	10.15	8.71	8.27	7.84
	φ	19.31	18.33	17.66	16.78	16.39	16.14	15.74
Zhang et al. (2017)	c	16.02	15.62	15.27	14.35	13.69	13.15	12.71
	φ	45.61	45.02	42.91	41.23	39.85	39.17	38.30
Zhou et al. (2012)	c	9.37	8.23	7.02	6.59	5.74	-	-
	φ	32.8	30.5	29.6	27.7	27.0	-	-
Liu et al. (2008)	c	14.05	13.04	-	11.88	-	-	10.64
	φ	39.39	38.37	-	36.57	-	-	35.25

where Z denotes the security margin, R denotes the anti-sliding force, and T denotes the sliding force.

Considering the uncertainty of the input variables, the performance function can be quantified by the reliability index (β) and failure probability (P_f). Let Z satisfy the normal distribution, hence β and P_f can be outlined as follows:

$$\beta = \mu_Z/\sigma_Z = (\mu_R - \mu_T)/\sqrt{\sigma_R^2 + \sigma_T^2 - 2\rho_{RT}\sigma_R\sigma_T} \quad (12)$$

$$P_f = P(Z < 0) = \Phi(0 - \mu_Z/\sigma_Z) = \Phi(-\beta) = 1 - \Phi(\beta) \quad (13)$$

where μ denotes the mean value, σ denotes the variance, Φ denotes the standard normal distribution function, and ρ_{RT} denotes the correlation coefficient of R and T, which characterizes the degree of linear correlation between R and T. When $|\rho_{RT} = 1|$, R and T are linearly related; when $|\rho_{RT} = 0|$, R is not related to T.

According to limit equilibrium method, the landslide is divided into designed number of slices, and let f_i replace $\tan\varphi_i$ to simplify the calculation. The security margin of the slice i is:

$$Z_i = R_i - T_i = N_i f_i + l_i c_i - T_i \quad (14)$$

Normally, the strength parameters are crucial internal factors affecting the calculation results for the defined landslide configuration (Miao et al. 2017). And the variability of the strength parameters under the periodic fluctuations of reservoir water level is more obvious. Therefore, c and φ are considered to be normally distributed and selected as random variables to establish the security margin function; then the local failure probability of the landslide can be calculated as follows:

$$\begin{cases} P_{f_i} = 1 - \Phi(\mu_{Z_i}/\sigma_{Z_i}) \\ \mu_{Z_i} = N_i\mu_{f_i} + l_i\mu_{c_i} - T_1 \\ \sigma_{Z_i} = N_i^2\sigma_{f_i} + l_i^2\sigma_{c_i} + 2N_il_iCov(f_i, c_i) \\ Cov(f_i, c_i) = \rho_{f_ici}\sqrt{\sigma_{f_i}\sigma_{c_i}} \end{cases} \quad (15)$$

where $Cov(f_i, c_i)$ denotes the covariance of f_i and c_i and $\rho_{f_i}c_i$ denotes the correlation coefficient of f_i and c_i.

Results

Weakening law

The periodic fluctuations of reservoir water level in the TGRA have formed an obvious hydro-fluctuation belt with a height of 30 m. Subsequently, the earth mass in this belt experiences alternating wetting-drying cycles, which inevitably leads to the degradation of its mechanical properties, especially strength parameters.

As mentioned above, the wetting-drying cycles test is conducted on the sliding zone soils of the Huangtupo Riverside Slump 1# to demonstrate the weakening law of the strength parameters. In the purpose of generalizing a more reliable weakening model and ulteriorly predicting the weakening of

Table 4 Fitting results of the strength parameters

Sources	Parameters	a	b	d	RMSE	R^2
Jiang et al. (2019)	c	0.10	0.91	0.49	0.75	0.991
	φ	0.78	0.22	0.075	0.18	0.956
Deng et al. (2017)	c	0.31	0.71	0.32	0.46	0.985
	φ	0.76	0.24	0.24	0.081	0.996
Zhang et al. (2017)	c	0.68	0.34	0.16	0.24	0.960
	φ	0.63	0.38	0.10	0.37	0.982
Zhou et al. (2012)	c	0.51	0.50	0.35	0.15	0.987
	φ	0.72	0.28	0.25	0.89	0.985
Liu et al. (2008)	c	0.67	0.33	0.21	0.079	0.998
	φ	0.86	0.14	0.23	0.067	0.999

Table 5 The values of strength parameters under wetting-drying cycles

Sliding zone soils	Parameters	Number of wetting-drying cycles								Coefficient of variation
		0	1	2	3	4	6	8	10	
Shallow	c	31.81	36.42	38.41	28.32	28.81	22.64	19.63	18.01	0.22
	φ	21.46	18.31	16.22	16.27	14.99	13.42	12.77	12.43	0.24
Deep	c	53.60	46.53	42.13	38.9	36.53	33.52	31.90	31.03	0.22
	φ	26.16	22.71	20.56	18.98	17.83	16.36	15.57	15.14	0.24

the strength parameters, several representative wetting-drying cycles results are also counted. These studies tested different types of soils or rocks in the TGRA, and the weakening results obtained were shown in Table 3.

Based on the existing experimental results and theoretical analysis, the weakening of strength parameters under wetting-drying cycles can be good characterized by an exponential function:

$$\omega(N) = \omega_0 \left(a + b e^{-Nd} \right) \quad (16)$$

where ω denotes the strength parameters, including c and φ; ω_0 denotes the initial value of parameters; N denotes the number of wetting-drying cycles; a denotes the residual weakening coefficient; b denotes the weakening proportionality coefficient; and d denotes the weakening law coefficient.

The weakening function is performed to fit the strength parameters, and the coefficients are obtained using the custom equation of Matlab toolbox with 95% confidence bounds. Besides, two statistical indices are introduced, namely the root mean square error (RMSE) and goodness of fit (R^2) to assess the fitting performance of the model (Liao et al. 2020b).

As shown in Table 4, the results confirm that the proposed weakening model has a high accuracy and is suitable for fitting the weakening of the strength parameters under wetting-drying cycles. In analogy, the model is conducted to fit the c and φ obtained in this study and predict the subsequent data. The coefficients of the weakening function are 0.56, 0.42, and 0.31, respectively. Considering the weakening of the shallow sliding zone and deep sliding zone soils synchronously, the strength parameters employed in the calculation under different number of wetting-drying cycles are shown in Table 5.

Long-term reliability analysis

Figure 7 shows that the Riverside Slump 1# is decomposed into multiple slices. Among them, the shallow sliding surface is divided into 20 slices, and the deep sliding surface is divided into 28 slices. The hydro-fluctuation belt affected by the reservoir scheduling is defined based on the demarcation of the corresponding phreatic lines when the reservoir water level is 145 and 175 m (Tang et al. 2015b). The number of weakening slices in the shallow sliding surface is eight and is four for the deep sliding surface. The basic calculation parameters are shown in Table 5 and Table 6 (Ni et al. 2013; Tang and Lu 2018). In particular, the weakening of the sliding zone soils in the hydro-fluctuation belt starts from the natural strength.

Prior to evaluating the reliability of the landslide, the factors of safety, F_s, under different wetting-drying cycles when the reservoir water level is 145 and 175 m are calculated, as shown in Fig. 8. Especially, when the number of wetting-drying cycles is 0, it is the initial state without considering the weakening of the strength parameters.

With the increase of wetting-drying cycles, the factor of safety decreases gradually, indicating that the landslide is developing toward instability. In addition, the stability of the shallow sliding surface is worse compared with the deep one at the same reservoir water level, and the stability of the reservoir water level at 175 m is worse than that at 145 m for the same sliding surface.

In more detail, taking the uncertainty of the strength parameters into account, the local failure probability of the shallow and deep surfaces is quantified.

As shown in Fig. 9, the local failure probability is roughly similar under different wetting-drying cycles, showing an

Table 6 Initial geotechnical parameters of the Riverside Slump 1#

Sliding zone soils	Weight (kN/m3)		Cohesion (kPa)		Internal friction angle (°)	
	Natural	Saturation	Natural	Saturation	Natural	Saturation
Shallow	20.3	21.2	31.8	26.7	21.46	18.25
Deep	20.3	21.2	53.6	48.4	26.16	23.72

Fig. 7 The calculation diagram of the Riverside Slump 1# considering the hydro-fluctuation belt
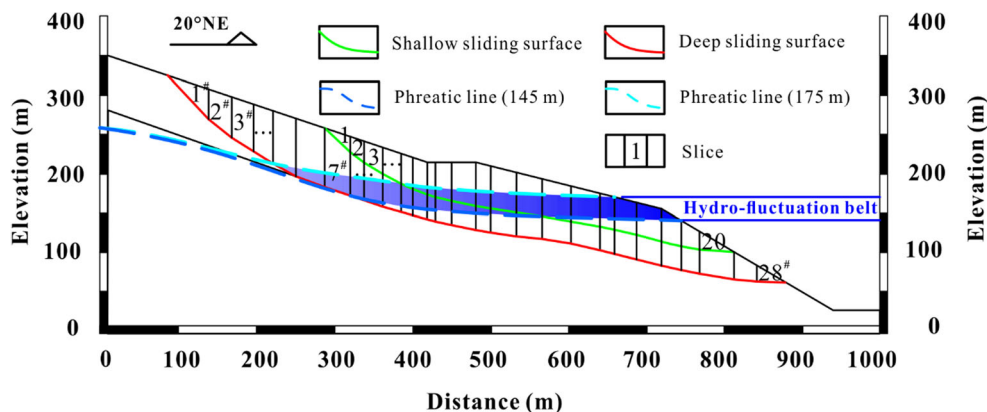
overall upward trend. This is because the weakening function employed in each cycle is the same, except for the first four cycles in the shallow sliding surface. Taking the shallow sliding surface at reservoir water level of 175 m as an example, the curve appears concave from the first to the fourth cycle. The reason behind the difference is that the c of the slices in the hydro-fluctuation belt has increased rather than decreased, which enhances the anti-sliding force of these slices.

The local failure probability of the landslide gradually rises as the number of wetting-drying cycles increases, and the shallow sliding surface is greater than that of the deep sliding surface. Taking the maximum local failure probability at the

Fig. 8 Factor of safety under different wetting-drying cycles, a reservoir water level of 145 m, b reservoir water level of 175 m

reservoir water level of 175 m as an example, the failure probability of the shallow slice increased from 5.06 to 22.92% after 10 cycles, and the deep slice increased from 4.50 to 8.43%. The intrinsic reason for this phenomenon is that there are eight shallow sliding slices located in the hydro-fluctuation belt, while there are only four deep sliding slices in this belt. As a result, the shallow sliding surface is more likely to be affected by the periodic reservoir operations.

The local failure probability at reservoir water level of 175 m is greater than that of 145 m. For example, the maximum failure probability of shallow sliding surface at the reservoir level of 175 m is 22.92%. By contrast, the failure probability is 17.85% when the reservoir water level is 145 m. Analogously, this result can be observed in the deep surface as well. It is worth noting that the conclusions obtained here assume that the reservoir water level remains stable without considering fluctuation, which means that the seepage field is steady when analyzing.
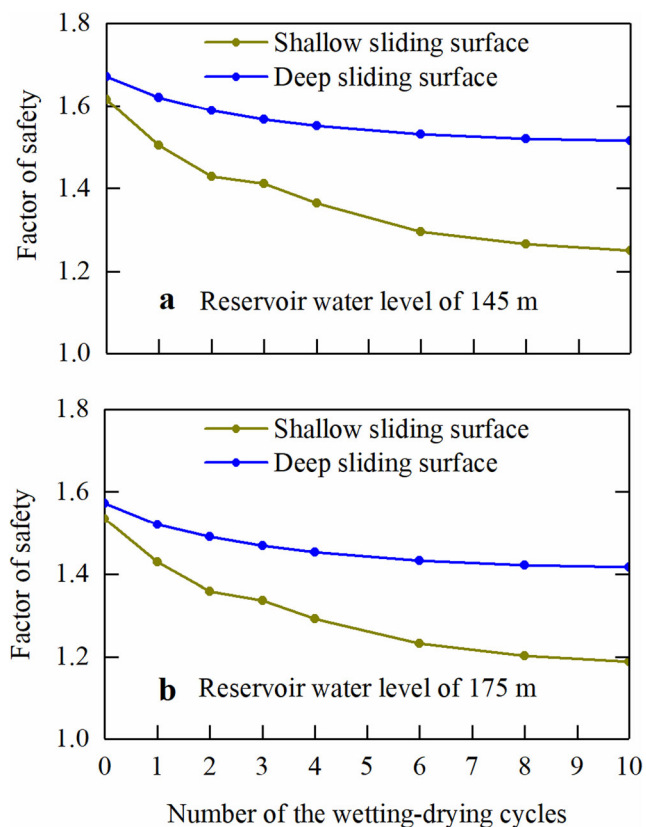
Discussion

Sensitivity of strength parameters

Under the periodic fluctuations of reservoir water level, the hydro-fluctuation belt experiences alternating wetting-drying cycles, resulting in the degradation of strength parameters and further affecting the stability of the landslide. In fact, the response of the landslide to the strength parameters is different. Generally, landslide is more sensitive to changes in φ, and this inference can be obtained implicitly from Fig. 9c. At the first cycle, c increased by 4.61 kPa compared to the initial state (0 wetting-drying cycle); on the contrary, φ decreased by 3.15°. Consequently, the maximum local failure probability increased by 2.01%.

More intuitively, the simple control variables method is conducted to analyze the sensitivity of the strength parameters. Taking the 10th slice in the shallow sliding surface when the reservoir water level is 175 m as a reference, c and φ are

Fig. 9 Local failure probability of the Riverside Slump 1#, **a** the shallow sliding surface at reservoir water level of 145 m, **b** the deep sliding surface at reservoir water level of 145 m, **c** the shallow sliding surface at reservoir water level of 175 m, **d** the deep sliding surface at reservoir water level of 175 m
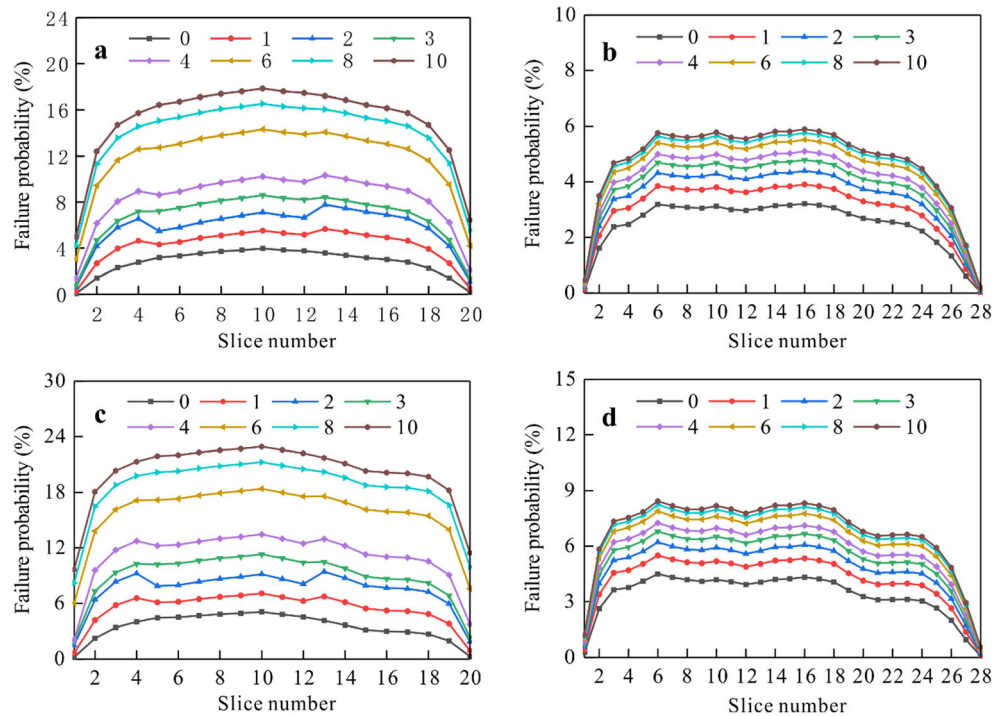
successively reduced by 5% each interval without considering wetting-drying cycles. The sensitivity results obtained by parameter analysis are shown in Fig. 10.

Figure 10 shows the results of failure probability when c and φ are varied. The inclination of the curves provides an indication regarding the sensitivity. Changing φ from 21.46 to 12.88° has more effect on the failure probability than changing the c from 31.81 to 19.09 kPa, despite the range being 40% in both cases. The curve of c is gentle, while the curve of φ shows a sharp rise indicating that the weakening of φ plays a growing role on the stability. Therefore, it is indispensable to notice the change of φ when evaluating the performance of the landslide.

Area of hydro-fluctuation belt

This study focuses on the sliding zone soils in the hydro-fluctuation belt affected by the repeated fluctuations of reservoir water level, which is mainly demarcated by the phreatic lines. In general, the demarcation can be acquired through the groundwater level monitoring or numerical simulation. There may be great errors and human factors in partitioning. In order to further investigate the effect of the area of hydro-fluctuation belt on the failure probability, three partitions containing different number of weakening shallow slices at reservoir water level of 175 m are calculated.

It can be drawn from Fig. 11a that the landslide tends to be more stable as the number of slices in the hydro-fluctuation belt increases. This is because under the existing model

configuration and reservoir water level, if the slices in the hydro-fluctuation belt increase, the saturated slices that use the saturation strength parameters will decrease. As a result, the stability of the landslide goes up, and the failure probability goes down. However, when the wetting-drying cycles are included, the response of the belt with more slices is more intense. Taking the 10th slice as an example, after 10 cycles, the failure probability is 30.94% when the 5 to 14 slices are weakened, while the failure probability is 16.1% when the 5 to 10 slices are weakened (Fig. 11b). The results show an obvious difference with the different number of weakening slices. We can therefore draw conclusion that the area of hydro-
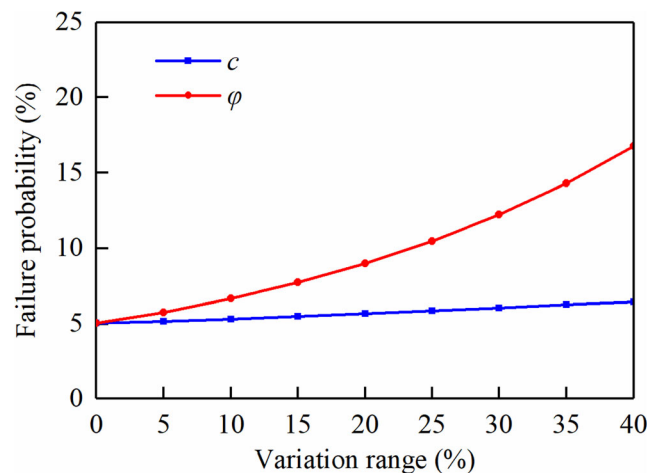

Fig. 10 The sensitivity of the shallow sliding surface to the strength parameters

Fig. 11 Local failure probability with different number of weakening slices, **a** under initial state, **b** under 10 wetting-drying cycles

Weakening slices: 5-10

Weakening slices: 5-12
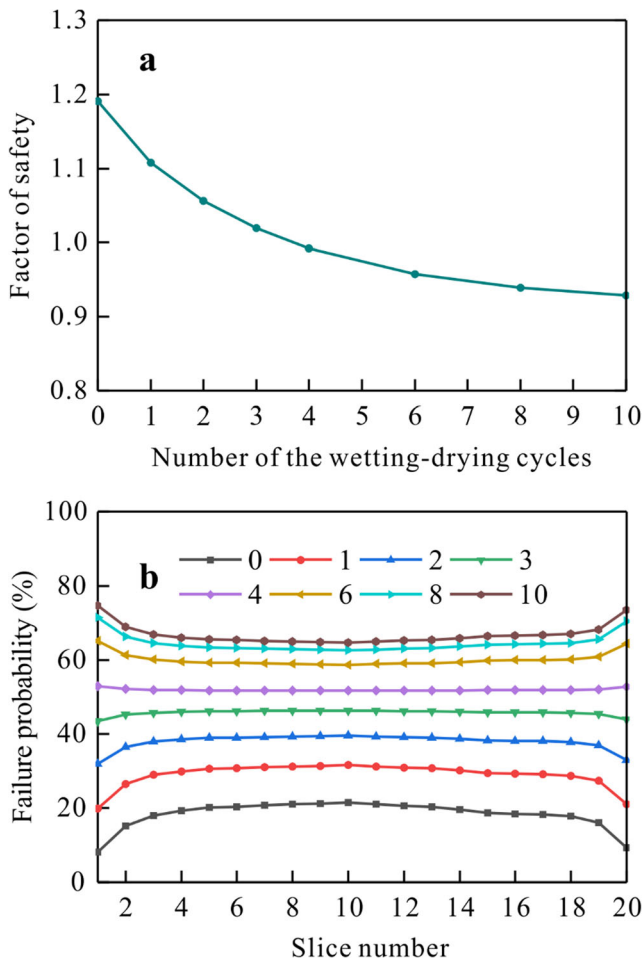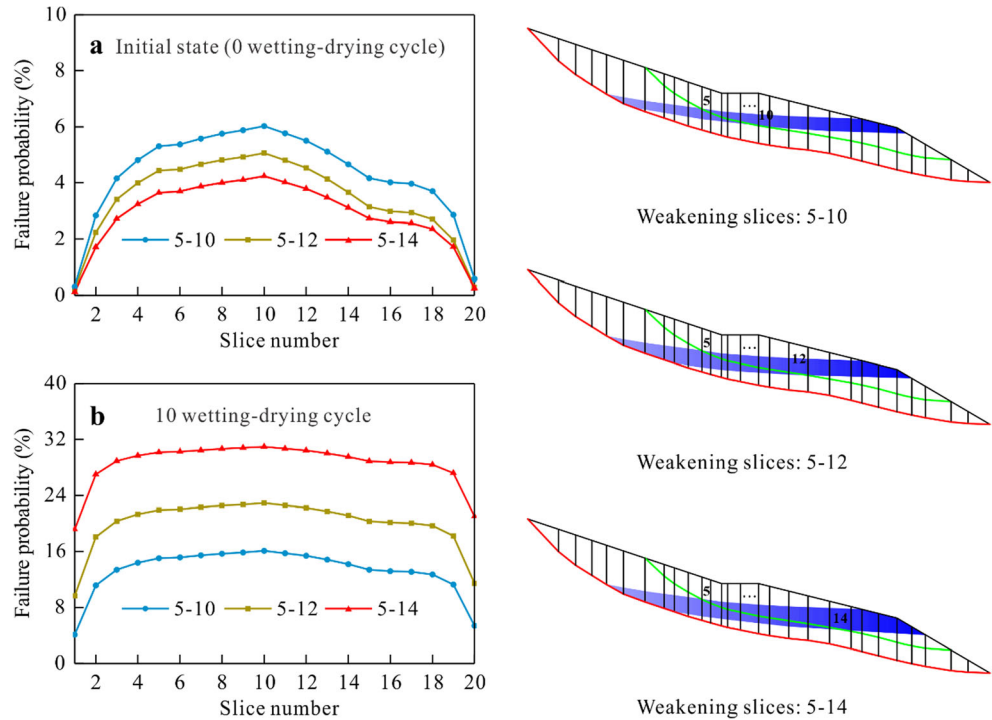
Weakening slices: 5-14

Fig. 12 Calculation results with the referenced strength parameters, **a** factor of safety, **b** local failure probability

fluctuation belt has a significant effect on the stability of the reservoir landslides. As a guide, the height difference of the reservoir water level should be closely monitored to avoid the formation of a widespread hydro-fluctuation belt in the actual reservoir operation.

Weakening model

Based on the wetting-drying cycles test implemented in the sliding zone soils, a weakening model is proposed to outline the degradation of strength parameters, which presents a high accuracy. But the results of the factor of safety seem to be inconspicuous. This is because the strength parameters and weakening model selected herein are obtained by sampling in the designed zone, the BR-3 of the Riverside Slump 1#. That is, the results of the test on a single zone are employed to represent the overall nature of the landslide. In fact, the strength parameters of the sliding surface at different positions may be different and the weakening law may not be similar as well, which can be known as spatial variability (Vanmarcke 2010). Even if the same weakening law is established, different parameter inputs may draw completely different conclusions. For example, we refer to the strength parameters, c_n=33 kPa, c_s=26 kPa, φ_n=16°, and φ_s=14°, used in the previous study (Ni et al. 2013) and analyze the stability of the shallow sliding surface at reservoir water level of 175 m according to the same weakening function. The factor of safety and local failure probability under different wetting-drying cycles are shown in Fig. 12.

Figure 12 shows that the factor of safety and local failure probability with the referenced strength parameters are quite different from the results obtained in this study due to different input parameters. By comparing the two sets of input parameters, it can be found that the input φ is relatively different. Thus, φ is the main reason for the different results, which is consistent with the sensitivity analysis results of strength parameters.

In addition, results of the wetting-drying cycles test, including the fitted model, can characterize the degradation of soil strength parameters, to a certain extent. The test has artificially produced the alternating process, reducing the time needed naturally via a more intense cycle than the actual one. Therefore, in the purpose of achieving a more accurate assessment and avoiding the errors caused by the single test, further more tests are needed to determine the strength parameters and weakening law at different positions.

Conclusions

The repeated fluctuations of reservoir water level have formed a representative hydro-fluctuation belt in the TGRA. The sliding zone soils in this belt experience alternating wetting-drying cycles under the periodic reservoir operations, leading to a degradation in its strength. The Huangtupo Riverside Slump 1#, a typical reservoir landslide with double sliding zones, is selected as the research object, and the following conclusions are reached in this study:

(1) The wetting-drying cycles test can well reflect the influence of the repeated reservoir operations on the sliding zone soils. The strength parameters gradually decrease with the continuous wetting-drying cycles, and an exponential function with clear physical and mathematical meanings is proposed to fit the degradation. The fitting achieves satisfactory results, and the proposed weakening model has the potential to be expanded by more tests to achieve a broad application in the reservoir area.

(2) The weakening of the sliding zone soils in the hydro-fluctuation belt has an adverse effect on the stability of the landslide. The shallow sliding surface presents a higher local failure probability, which reflects a stronger response to the long-term reservoir operations. The primary reason behind this result is that the area of the hydro-fluctuation belt where the shallow sliding surface located is greater than that of the deep sliding surface.

(3) The sensitivity of the landslide response to strength parameters is different, and φ is much greater than c. When φ decreases, the local failure probability increases dramatically, which means that the weakening of φ plays a growing role on the stability. On the other hand, c has

little effect on the local failure probability, showing an approximately linear relationship with low slope.

(4) The area of the hydro-fluctuation belt directly affects the stability of the landslide, which should be paid more attention to guide the scheduling of reservoir water level. The methods of dividing the weakening area by the hydro-fluctuation belt and simulating the repeated reservoir operations by the wetting-drying cycles test provide an insightful idea for analyzing the long-term stability of reservoir landslides in the TGRA.

(5) It would be wise to complete the landslide instrumentation by monitoring the water content of the soils at the level of the failure surfaces, according to the piezometric levels. This could only be done through boring and sampling for different piezometric levels in the landslide in response to fluctuations in the level of the reservoir.

References

Barla G, Paronuzzi P (2013) The 1963 Vajont landslide: 50th anniversary. Rock Mech Rock Eng 46(6):1267–1270. https://doi.org/10.1007/s00603-013-0483-7

Bishop AW (1955) The use of the slip circle in the stability analysis of slopes. Geotechnique 5(1):7–17. https://doi.org/10.1680/geot.1955.5.1.7

Chen ZY, Du JF, Yan JJ, Sun P, Li KP, Li YL (2019) Point estimation method: Validation, efficiency improvement, and application to embankment slope stability reliability analysis. Eng Geol 263:105232. https://doi.org/10.1016/j.enggeo.2019.105232

Deng HF, Zhou ML, Li JL, Sun XS, Huang YL (2016) Creep degradation mechanism by water-rock interaction in the red-layer soft rock. Arab J Geosci 9:42–57. https://doi.org/10.1007/s12517-016-2604-6

Deng HF, Xiao Y, Fang JC, Zhang HB, Wang CXJ, Cao Y (2017) Shear strength degradation and slope stability of soils at hydro-fluctuation belt of river bank slope during drying-wetting cycle. Rock Soil Mech 38(9):2629–2638 (**In Chinese**)

Du J, Yin KL, Lacasse S (2013) Displacement prediction in colluvial landslides, Three Gorges Reservoir, China. Landslides 10(2):203–218. https://doi.org/10.1007/s10346-012-0326-8

Duman TY (2009) The largest landslide dam in Turkey: Tortum landslide. Eng Geol 104(1-2):66–79. https://doi.org/10.1016/j.enggeo.2008.08.006

Fenton GA, Naghibi F, Griffiths DV (2016) On a unified theory for reliability-based geotechnical design. Comput Geotech 78:110–122. https://doi.org/10.1016/j.compgeo.2016.04.013

Gullà G, Mandaglio MC, Moraci N (2006) Effect of weathering on the compressibility and shear strength of a natural clay. Can Geotech J 43(6):618–625. https://doi.org/10.1139/T06-028

Gutiérrez F, Lucha P, Galve JP (2010) Reconstructing the geochronological evolution of large landslides by means of the trenching

technique in the Yesa Reservoir (Spanish Pyrenees). Geomorphology 124(3-4):124–136. https://doi.org/10.1016/j.geomorph.2010.04.015

Huang RQ (2009) Some catastrophic landslides since the twentieth century in the southwest of China. Landslides 6(1):69–81. https://doi.org/10.1007/s10346-009-0142-y

Huang RQ (2012) Mechanisms of large-scale landslides in China. Bull Eng Geol Environ 71(1):161–170. https://doi.org/10.1007/s10064-011-0403-6

Janbu N (1957) Earth pressure and bearing capacity calculations by generalized procedure of slices. In: The proceeding of the 4th international conference on soil mechanics and foundation engineering, London, vol 2, pp 207–212

Jiang QQ, Liu LL, Jiao YY, Wang H (2019) Strength properties and microstructure characteristics of slip zone soil under wetting–drying cycles. Rock Soil Mech 40(3):1005–1012 (**In Chinese**)

Jiao YY, Song L, Tang HM, Li YA (2014) Material weakening of slip zone soils induced by water level fluctuation in the ancient landslides of Three Gorges Reservoir. Adv Mater Sci Eng 2014:9. https://doi.org/10.1155/2014/202340

Juang CH, Gong WP, Martin JR, Chen QS (2018) Model selection in geological and geotechnical engineering in the face of uncertainty - Does a complex model always outperform a simple model? Eng Geol 242:184–196. https://doi.org/10.1016/j.enggeo.2018.05.022

Kirschbaum D, Stanley T, Zhou Y (2015) Spatial and temporal analysis of a global landslide catalog. Geomorphology 249:4–15. https://doi.org/10.1016/j.geomorph.2015.03.016

Li DQ, Zhang FP, Cao ZJ, Zhou W, Phoon KK, Zhou CB (2015) Efficient reliability updating of slope stability by reweighting failure samples generated by Monte Carlo simulation. Comput Geotech 69:588–600. https://doi.org/10.1016/j.compgeo.2015.06.017

Li C, Tang HM, Han DW, Zou ZX (2019) Exploration of the creep properties of undisturbed shear zone soil of the Huangtupo landslide. Bull Eng Geol Environ 78(2):1237–1248. https://doi.org/10.1007/s10064-017-1174-5

Liao K, Wu YP, Miao FS, Li LW, Xue Y (2020a) Time-varying reliability analysis of Majiagou landslide based on weakening of hydro-fluctuation belt under wetting-drying cycles. Landslides 18:1–14. https://doi.org/10.1007/s10346-020-01496-2

Liao K, Wu YP, Miao FS, Li LW, Xue Y (2020b) Using a kernel extreme learning machine with grey wolf optimization to predict the displacement of step-like landslide. Bull Eng Geol Environ 79(2):673–685. https://doi.org/10.1007/s10064-019-01598-9

Liu XR, Fu Y, Wang YX, Huang LW, Qin XY (2008) Deterioration rules of shear strength of sand rock under water-rock interaction of reservoir. Chin J Geotech Eng 30(9):1298–1302 (**In Chinese**)

Lu S, Tang HM, Zhang YQ, Gong WP, Wang LQ (2018) Effects of the particle-size distribution on the micro and macro behavior of soils: fractal dimension as an indicator of the spatial variability of a slip zone in a landslide. Bull Eng Geol Environ 77(2):665–677. https://doi.org/10.1007/s10064-017-1028-1

Miao FS, Wu YP, Xie YH, Yu F, Peng LJ (2017) Research on progressive failure process of Baishuihe landslide based on Monte Carlo model. Stoch Env Res Risk A 31(7):1683–1696. https://doi.org/10.1007/s00477-016-1224-8

Miao FS, Wu YP, Li LW, Tang HM (2020) Weakening laws of slip zone soils during wetting–drying cycles based on fractal theory: a case study in the Three Gorges Reservoir (China). Acta Geotech 15(7):1909–1923. https://doi.org/10.1007/s11440-019-00894-8

Micu M, Bălteanu D (2013) A deep-seated landslide dam in the Siriu Reservoir (Curvature Carpathians, Romania). Landslides 10:323–329. https://doi.org/10.1007/s10346-013-0382-8

Morgenstern NR, Price VE (1965) The analysis of the stability of general slip surfaces. Geotechnique 5(1):79–93. https://doi.org/10.1680/geot.1965.15.1.79

Ng CWW, Xu J, Yung SY (2009) Effects of wetting-drying and stress ratio on anisotropic stiffness of an unsaturated soil at very small strains. Can Geotech J 46(9):1062–1076. https://doi.org/10.1139/T09-043

Ni WD, Tang HM, Hu XL, Wu YP, Su AJ (2013) Research on deformation and stability evolution law of Huangtupo riverside slump-mass No. I. Rock Soil Mech 34(10):2961–2970 (**In Chinese**)

Paronuzzi P, Rigo E, Bolla A (2013) Influence of filling-drawdown cycles of the Vajont reservoir on Mt. Toc slope stability. Geomorphology 191:75–93. https://doi.org/10.1016/j.geomorph.2013.03.004

Pasculli A, Sciarra N, Esposito L, Esposito AW (2017) Effects of wetting and drying cycles on mechanical properties of pyroclastic soils. Catena 156:113–123. https://doi.org/10.1016/j.catena.2017.04.004

Peng X, Li DQ, Cao ZJ, Gong W, Juang CH (2017) Reliability-based robust geotechnical design using Monte Carlo Simulation. Bull Eng Geol Environ 76(3):1217–1227. https://doi.org/10.1007/s10064-016-0905-3

Penna D, Brocca L, Borga M, Dalla Fontana G (2013) Soil moisture temporal stability at different depths on two alpine hillslopes during wet and dry periods. J Hydrol 477:55–71. https://doi.org/10.1016/j.jhydrol.2012.10.052

Phoon KK, Ching J, Chen JR (2013) Performance of reliability-based design code formats for foundations in layered soils. Comput Struct 126:100–106. https://doi.org/10.1016/j.compstruc.2012.12.023

Sarma SK (1979) Stability analysis of embankments and slopes. J Geotech Eng Div 105(12):1511–1524

Spencer E (1968) The analysis of the stability of general slip surfaces. Geotechnique 18(1):92–93. https://doi.org/10.1680/geot.1968.18.1.92

Tang HM, Lu S (2018) Research on the spatial distribution of slip zone of Huangtupo landslide in Three Gorges Reservoir area. J Eng Geol 26(1):129–136 (In Chinese)

Tang HM, Li CD, Hu XL, Su AJ, Wang LQ, Wu YP, Criss R, Xiong CR, Li YA (2015a) Evolution characteristics of the Huangtupo landslide based on in situ tunneling and monitoring. Landslides 12(3):511–521. https://doi.org/10.1007/s10346-014-0500-2

Tang HM, Li CD, Hu XL, Wang LQ, Criss R, Su AJ, Wu YP, Xiong CR (2015b) Deformation response of the Huangtupo landslide to rainfall and the changing levels of the Three Gorges Reservoir. Bull Eng Geol Environ 74(3):933–942. https://doi.org/10.1007/s10064-014-0671-z

Tang CS, Wang DY, Shi B, Li J (2016) Effect of wetting-drying cycles on profile mechanical behavior of soils with different initial conditions. Catena 139:105–116. https://doi.org/10.1016/j.catena.2015.12.015

Tang HM, Wasowski J, Juang CH (2019) Geohazards in the three Gorges Reservoir Area, China – lessons learned from decades of research. Eng Geol 261:105267. https://doi.org/10.1016/j.enggeo.2019.105267

Vanmarcke EH (2010) Random fields: analysis and synthesis. World Scientific Publishing Co. Pte. Ltd., Singapore

Wang JE, Xiang W, Lu N (2014) Landsliding triggered by reservoir operation: a general conceptual model with a case study at Three Gorges Reservoir. Acta Geotech 9(5):771–788. https://doi.org/10.1007/s11440-014-0315-2

Wang S, Wu W, Wang JE, Yin ZY, Cui DS, Xiang W (2018a) Residual-state creep of clastic soil in a reactivated slow-moving landslide in the Three Gorges Reservoir Region, China. Landslides 15(12):2413–2422. https://doi.org/10.1007/s10346-018-1043-8

Wang JE, Su AJ, Liu QB, Xiang W, Yeh HF, Xiong CR, Zou ZX, Zhong C, Liu JQ, Cao S (2018b) Three-dimensional analyses of the sliding surface distribution in the Huangtupo No. 1 riverside sliding mass in the Three Gorges Reservoir area of China. Landslides 15(7):1425–1435. https://doi.org/10.1007/s10346-018-1003-3

Wen BP, Aydin A, Aydin NS, Li RR, Chen HY, Xiao SD (2007) Residual strength of slip zones of large landslides in the Three Gorges area, China. Eng Geol 93(3-4):82–98. https://doi.org/10.1016/j.enggeo.2007.05.006

Yao WM, Li CD, Zhan HB, Zhang HW, Chen WQ (2020) Probabilistic multi-objective optimization for landslide reinforcement with stabilizing piles in Zigui Basin of Three Gorges Reservoir region, China. Stoch Env Res Risk A 34:807–824. https://doi.org/10.1007/s00477-020-01800-5

Yin YP, Huang BL, Wang WP, Wei YJ, Ma XH, Ma F, Zhao CJ (2016) Reservoir-induced landslides and risk control in Three Gorges Project on Yangtze River, China. J Rock Mech Geotech Eng 8(5): 577–595. https://doi.org/10.1016/j.jrmge.2016.08.001

Zhang JY, Wan LP, Pan HY, Li JL, Luo ZS, Deng HF (2017) Long-term reliability of bank slope considering characteristics of water-rock interaction. Chin J Geotech Eng 39(10):1851–1858 (**In Chinese**)

Zhou SL, Liu XQ, Shang MF, Li Y (2012) Time-varying stability analysis of mudstone reservoir bank based on water-rock interaction. Rock Soil Mech 33(7):1933–1939 (**In Chinese**)

Zhu DY, Qian QH, Zhou ZS, Zheng HT (1999) Critical slip field of slope based on the assumption of unbalanced thrust method. Chin J Rock Mech Eng 18(6):667–670 (**In Chinese**)